



OPEN Natural fatal infection of Tembusu virus in bottlenose dolphins in Thailand

Chutchai Piewbang^{1,2,7}, Le Yi^{3,7}, Aisyah Nikmatuz Zahro^{1,2,4}, Panida Poonsin^{1,2}, Panitnan Panyathi^{1,2}, Tanit Kasantikul⁵, Nathamon Kosoltanapiwat⁶, Biao He³ & Somporn Techangamsuwan^{1,2}✉

Interspecies transmission of viruses poses significant risks to animal and human health. Tembusu virus (TMUV), an emerging flavivirus, is primarily associated with avian diseases. This study reports the first documented natural infection of TMUV in mammals, specifically zoo dolphins in Thailand, offering insights into its evolution, transmission dynamics, and zoonotic potential. In July 2023, three bottlenose dolphins developed neurological symptoms and died. Postmortem analyses, including histopathology, immunohistochemistry, high-throughput sequencing, and transmission electron microscopy, confirmed TMUV infection. Viral loads were high in brain and lung tissues, followed by kidney and spleen whereas the TMUV antigen was identified in only brain tissue. TMUV was localized in neurons and astroglia cells, and immunohistochemistry revealed CD3-positive T lymphocyte perivascular cuffing in the brain. Phylogenetic analysis placed the dolphin TMUV strains within cluster 3, related to strains found in mosquitoes in China. Retrospective analysis of dolphin samples from 2019 confirmed persistent TMUV circulation. Viral isolation on Vero cells showed characteristic cytopathic effects, and transmission electron microscopy revealed enveloped virions. This study highlights the virus's ability to infect diverse hosts, including mammals. The findings underscore the need for continuous surveillance and a One Health approach to mitigate emerging viral threats.

Keywords Dolphin, Flavivirus, Interspecies transmission, Tembusu virus, Thailand

Interspecies transmission of viruses has been reported on many occasions, often due to close contact or evolutionary proximity among susceptible hosts^{1,2}. The viral replication in hosts is a complex mechanism involving various interactions, and coevolution between viral pathogens and host also shapes infection patterns³. Infections can occur when infective elements are transmitted to hosts with coevolutionary or genetic proximity to the natural reservoirs⁴, even if the new host does not support sustained transmission. Several viruses, such as emerging influenza viruses and coronaviruses, are known to infect various types of hosts^{2,5}. In addition to these, flaviviruses exhibit a broad host range, often involving intermediate mosquitoes or arthropods. The *Flaviviridae* family contains four genera: *Orthoflavivirus*, *Pestivirus*, *Hepacivirus*, and *Pegivirus*⁶. Over 50% of known orthoflaviviruses cause disease in humans, including Japanese encephalitis virus (JEV), West Nile virus (WNV), and Dengue virus (DENV). Others, such as Tembusu virus (TMUV) and Usutu virus, are associated with diseases in wild and domestic animals⁶.

Tembusu virus (TMUV) is an emerging flavivirus that has been shown to cause decreased egg production and severe neurological disorders in ducks⁷. TMUV-related viruses were first identified in mosquitoes in Malaysia in the 1950s⁸, with sporadic reports in broiler chickens and ducks in Malaysia and China, respectively⁹. In 2010, TMUV outbreaks were massively reported in duck farms in Thailand and China, leading to significant

¹Department of Pathology, Faculty of Veterinary Science, Chulalongkorn University, Bangkok 10330, Thailand.

²Animal Virome and Diagnostic Development Research Unit, Faculty of Veterinary Science, Chulalongkorn University, Bangkok, Thailand. ³State Key Laboratory of Pathogen and Biosecurity, Key Laboratory of Jilin Province for Zoonosis Prevention and Control, Changchun Veterinary Research Institute, Chinese Academy of Agricultural Sciences, Changchun, Jilin Province, China. ⁴The International Graduate course of Veterinary Science and Technology (VST), Faculty of Veterinary Science, Chulalongkorn University, Bangkok, Thailand. ⁵Department of Pathobiology and Diagnostic Investigation, College of Veterinary Medicine, Michigan State University, East Lansing, MI, USA. ⁶Department of Microbiology and Immunology, Faculty of Tropical Medicine, Mahidol University, Bangkok, Thailand. ⁷Chutchai Piewbang and Le Yi contributed equally to this work. ✉email: somporn.t@chula.ac.th

economic losses^{7,10,11}. Clinical manifestations include egg-drop syndrome and peritonitis, with neurological signs occasionally reported in infected young birds^{12,13}.

TMUV is a positive-sense, single-stranded RNA virus belonging to the *Orthoflavivirus* genus, with an approximately 11 kb genome⁶. Among its structural proteins, the E gene is crucial for encoding a virulent protein involved in viral attachment, plasma membrane fusion, and replication¹⁴. This gene also determines the virus's cellular tropism and is used for classifying TMUV into clusters 1 to 3¹⁵. While clusters 1 and 2 have been predominantly reported in Thailand and China, respectively, information on TMUV cluster 3 is limited and was first officially reported in 2019 in Thailand¹⁶. However, surveillance of flaviviruses in mosquitoes in Thailand in 1992 and 2002 revealed that TMUV cluster 3 was already present¹⁷. This evidence suggests that TMUV cluster 3 may represent an earlier lineage in the evolutionary history of TMUV, potentially contributing to the diversity observed in other clusters. Additionally, TMUV cluster 3 appears to exhibit a broader host range compared to other clusters, identified in mosquitoes^{17,18}, ducks¹⁶, chickens^{19,20}, sparrows²¹, and geese^{22,23}.

Apart from affecting various bird species, there is evidence that TMUV can infect mammalian hosts. Inoculations of TMUV in BALB/c and Kunming mice exhibit neurological deficits and systemic infection, with TMUV titers and TMUV-specific neutralizing antibodies recovered^{24–26}. Infected mice showed significant non-suppurative encephalitis, and TMUV proteins were detected in neurons and glial cells^{24,26,27}. Various mammalian- and human-derived cell lines are also permissive to TMUV infection²⁸. Additionally, neutralizing antibodies against TMUV were detected in the sera of humans, and TMUV RNA was identified in throat swabs of duck farm workers in China²⁹. This suggests zoonotic potential and the ability to infect mammals, though the possibility of transmission through intermediate hosts, such as mosquitoes, cannot be excluded. Although flaviviruses are predominantly found in terrestrial species³⁰, infections or endogenous flaviviral elements have been reported in aquatic and marine species, especially in marine mammals^{30–32}. In this study, we identified TMUV as the cause of non-suppurative encephalitis in zoo dolphins in Thailand. This is the first report of natural TMUV infection in mammals, providing significant insights into the virus's evolution, circulation patterns, and interspecies transmission dynamics.

Materials and methods

Ethics

This study was approved by the Institutional Animal Care and Use Committee (IACUC) of the Faculty of Veterinary Science, Chulalongkorn University, Thailand (approval No. 2431048). All methods performed in this study were carried out in accordance with the institutional and ARRIVE guidelines and regulations.

Animals and retrospective samples

In July 2023, three male, captive-bred common bottlenose dolphins (*Tursiops truncatus*), housed in a private zoo in Thailand, developed progressive neurological signs. The dolphins were kept together in the same 550-square-meter aquarium pond with a water depth of 3.5 m and a total volume of approximately 2000 cubic meters, with a four-hour turnover flow and filtration system. They were not co-housed with any other animal species.

The first dolphin (case no. 1) initially presented with decreased appetite for one week, followed by decreased coordination and body tremors. Upon clinical deterioration, case no. 1 was separated and quarantined in a separate pond. Initial hematology and biochemistry results were within normal limits. During quarantine, the two other dolphins (case nos. 2 and 3) developed similar neurological signs approximately two weeks later, and their condition progressively worsened over the following weeks. Supportive treatment, including antibiotic therapy (fluoroquinolone, ceftriaxone, or a combination of both), was administered to all three dolphins. Despite intensive management, case no. 1 succumbed within a few weeks of symptom onset, followed by case nos. 2 and 3 after prolonged supportive care. The total clinical course lasted approximately one month from the onset of signs in case no. 1 to the deaths of all three dolphins.

The necropsies were performed at the zoo by the attending veterinarians, and only selected tissues were submitted for histopathology and viral investigations; therefore, a detailed gross pathological examination was not available for evaluation. Tissues from multiple organs, including the brain, lungs, kidneys, spleen, heart, pancreas, intestine, and liver, were collected and preserved as formalin-fixed, paraffin-embedded (FFPE) samples. Additionally, fresh-frozen tissues from the same organs of case nos. 1–3 and swab samples from the rectum and blowhole cavity of case no. 1 were collected and stored at -80°C until analysis. FFPE samples underwent routine histological examination with hematoxylin and eosin (H&E) staining, while fresh-frozen tissues were submitted for viral molecular diagnostics at the Department of Pathology, Faculty of Veterinary Science, Chulalongkorn University.

To further investigate the presence of TMUV in dolphins, archival samples from six captive-bred bottlenose dolphins (*T. truncatus*) (case nos. 4–9) and three captive-bred Indo-Pacific humpback dolphins (*Sousa chinensis*) (case nos. 10–12), which had died from various or unknown causes between 2015 and 2023, were retrospectively examined. Since the objective was to determine the presence of TMUV in any available dolphin samples, all archived dolphin cases in our department were included without exclusion criteria. These archival samples, stored at the Department of Pathology, Faculty of Veterinary Science, Chulalongkorn University, as well as private laboratories in Bangkok, Thailand, included both fresh-frozen and FFPE samples. A detailed summary of all investigated cases is provided in Table 1.

Nucleic acid extraction and routine virologic testing

The fresh tissue samples, approximately 5 g each, were homogenized with 0.5X phosphate-buffered saline (PBS) solution using an automated homogenizer (Bead Ruptor 12, Omni International, GA, USA). The supernatant from the homogenized tissues and swabs was collected and submitted for nucleic acid extraction using a commercial extraction kit and an automated nucleic acid extraction machine (QIAcube, Qiagen, Hilden,

Case no.	Species	Age (year) /Sex	Date of collection	Tissues	Detection of TMUV			Morphological diagnosis(es)
					RT-qPCR (Ct value)	IHC	Virus isolation [‡]	
1	<i>T. truncatus</i>	20/ Male	2023	Brain	30.12	+	CPE*	1. Moderate perivascular non-suppurative encephalitis and mild perivascular edema with multifocal gliosis. 2. Marked multifocal suppurative pyelonephritis and marked multifocal lymphoplasmacytic interstitial nephritis with marked interstitial fibrosis 3. Regional pulmonary fibrosis; diffuse pulmonary congestion and edema
				Kidney	31.17	–	NA	
				Lung	29.18	–	CPE*	
				Spleen	33.42	–	NA	
				Rectal swab	–	NA	NA	
				Blowhole swab	35.12	NA	NA	
2	<i>T. truncatus</i>	15/ Male	2023	Brain	31.42	+	NA	1. Moderate perivascular non-suppurative encephalitis and mild perivascular edema with multifocal gliosis. 2. Renal congestion
				Kidney	36.75	–	NA	
				Lung	–	–	NA	
3	<i>T. truncatus</i>	17/ Male	2023	Brain	31.18	+	NA	Brain congestion with minimal to mild non-suppurative encephalitis and moderate perivascular edema
				Kidney	–	–	NA	
				Lung	–	–	NA	
4	<i>T. truncatus</i>	Adult/ Female	2022	Brain	–	–	NA	1. Moderate brain congestion 2. Severe pulmonary congestion
				Kidney	–	NA	NA	
				Lung	–	NA	NA	
				Liver	–	NA	NA	
5	<i>T. truncatus</i>	Adult/ Male	2022	Brain	–	-	NA	Severe tissue autolysis
				Kidney	–	NA	NA	
				Lung	–	NA	NA	
6	<i>T. truncatus</i>	Adult/Male	2020	Brain	–	NA	NA	Severe pulmonary fibrosis with extraintestinal larva migration
				Lymph nodes	–	–	NA	
				Lung	–	–	NA	
7*	<i>T. truncatus</i>	15/ Female	2019	Brain	35.41	+	NA	Moderate non-suppurative encephalitis and gliosis
				Kidney	–	–	NA	
				Lung	–	–	NA	
				Liver	–	NA	NA	
8*	<i>T. truncatus</i>	Unknown/ Male	2019	Brain	34.21	+	NA	1. Moderate non-suppurative encephalitis and gliosis, with severe perivascular cuffing 2. Non-suppurative meningitis
				Kidney	–	–	NA	
				Lung	–	–	NA	
				Liver	–	NA	NA	
9*	<i>T. truncatus</i>	Unknown/ Female	2019	Brain	34.32	+	NA	Mild gliosis with mild non-suppurative perivascular cuffing
				Kidney	–	–	NA	
				Lung	–	–	NA	
				Lymph nodes	–	–	NA	
10	<i>S. chinensis</i>	45/ Male	2016	Brain	–	–	NA	1. Squamous cell carcinomas with metastasis 2. Moderate pulmonary congestion
				Kidney	–	NA	NA	
				Lung	–	–	NA	
				Lymph nodes	–	NA	NA	
				Skin	–	NA	NA	
11	<i>S. chinensis</i>	45/ Female	2016	Brain	–	-	NA	Squamous cell carcinomas with metastasis
				Kidney	–	-	NA	
				Lung	–	-	NA	
				Lymph nodes	–	NA	NA	
				Skin	–	NA	NA	
Continued								

Case no.	Species	Age (year) /Sex	Date of collection	Tissues	Detection of TMUV			Morphological diagnosis(es)
					RT-qPCR (Ct value)	IHC	Virus isolation [‡]	
12	<i>S. chinensis</i>	45/ Female	2015	Brain	–	–	NA	Squamous cell carcinomas with metastasis
				Kidney	–	–	NA	
				Lung	–	NA	NA	
				Lymph nodes	–	NA	NA	
				Skin	–	NA	NA	

Table 1. Investigation of Tembusu virus (TMUV) infection in dolphins. CPE: cytopathic effect; Ct: cycle threshold; IHC: immunohistochemistry; NA: Not determine; RT-qPCR: quantitative reverse-transcription polymerase chain reaction; TMUV: Tembusu virus. [‡] Virus isolation was performed on pooled brain and lung homogenization. *Archival samples that had only formalin-fixed, paraffin-embedded (FFPE) samples. RT-qPCR is performed on the nucleic acid extraction of the FFPE shaving.

Germany). The obtained nucleic acids were then quantified and qualified using a 260/280 ratio spectrophotometer (NanodropLite, Thermo Fisher Scientific Inc., Waltham, MA, USA). Subsequently, the samples were subjected to virologic testing panels using either conventional (c) or quantitative (q), reverse transcription (RT) polymerase chain reaction (PCR), targeting various viral families. The viral targets of the PCR panels included paramyxovirus^{33,34}, herpesvirus³⁵, poxvirus³⁶, and papillomavirus³⁷, following previously described protocols and primers. Furthermore, specific PCR tests against morbillivirus³⁴ and *Toxoplasma gondii*³⁸ were performed. Routine immunohistochemistry (IHC) targeting canine/phocine morbillivirus was also conducted on the FFPE-brain and lung sections, following a previous described protocol³⁹. The archival samples, which included either fresh-frozen or FFPE samples, were subjected to routine RT-qPCR detection and IHC analysis as described above. For the archival samples without fresh-frozen tissue, RNA extraction was performed using RNeasy FFPE extraction kit (Qiagen, Hilden, Germany) on shaved FFPE slides, following previously described protocols⁴⁰.

High-throughput sequencing and genome analysis

The supernatant obtained from the homogenized fresh-frozen lung and brain tissues of case no.1 was pooled, filtered with a 0.4-µm cellulose membrane, and dried on Fast Technology for Analysis (FTA) cards (QIACard FTA Indicating Classic, Qiagen, Hilden, Germany). The cards were then shipped for metagenomic analysis using high-throughput sequencing. The DNA library was constructed using the NEBNext® Ultra Directional RNA Library Prep Kit (NEB) and subsequently sequenced on an Illumina NovaSeq 6000. The generated raw data were trimmed, analyzed, and assembled. Meta-transcriptomic (MTT) sequencing combined with multiple displacement amplification (MDA) was employed to profile the viral metagenomes⁴¹. MetaSPAdes and Megahit were used for genome assembly. The complete TMUV genome sequence generated was then aligned with previously identified TMUV sequences available in the GenBank database using the BLASTn algorithm. The alignment sequences were used for genome analysis. Pairwise nucleotide and deduced amino acid sequence identities were calculated using the BioEdit software package v. 7.2. Based on the Bayesian criterion, the general-time reversible (GTR) model and Tamura and Nei 1993 (TN93) models were selected for phylogenetic tree construction based on complete nucleotide and amino acid sequences. Phylogenetic trees were constructed using MEGA software v. 11.

Viral loads quantification of TMUV in dolphins

Following the results from high-throughput sequencing, nucleic acid samples extracted from various organs including brain, lungs, kidneys, spleen, heart, pancreas, intestine, and liver of case nos. 1–3 were tested to detect and quantify the presence of TMUV. A SYBR Green-based RT-qPCR specific to TMUV cluster 3 was performed. Briefly, 2 µl of extracted nucleic acids were combined with a RT-qPCR reaction mix (qPCR BIO SyGreen 1-step kit-GO Lo-Lox, PCR BIOSYSTEMS, London, UK) and previously described TMUV primers⁴². The RT-qPCR protocols included an RT step at 45 °C for 10 min, followed by polymerase activation at 95 °C for 2 min, and 40 cycles of denaturation at 95 °C for 10 s and annealing at 60 °C for 30 s. Melt curve analysis was performed from 70 to 95 °C, increasing by 1 °C increments, with acquisition on the green melt channel. Samples that presented signals after 38 cycles were considered negative. A non-template tube was used as a negative control. The obtained cycle threshold (Ct) value was used to estimate the amounts of TMUV. The RT-qPCR products were then subjected to Sanger sequencing (Celegics, South Korea), to confirm the presence of TMUV. The obtained sequences were subsequently used for phylogenetic tree construction using the Maximum Likelihood (ML) method implemented in MEGA software v. 11, with 1000 bootstrap replicates. To determine the amino acid sequence mutations of the TMUV E gene, conventional PCR targeting the complete E gene was performed using the protocols and primers described previously²³. The resulting PCR products were subjected to Sanger sequencing (U2BIO, South Korea). The deduced amino acid sequences of the E gene were then compared to previously described TMUV strains available in the GenBank database to identify mutations.

Virus isolation

Virus isolation was performed using Vero cells (ATCC CCL81). The cells were grown in Minimum Essential Medium (MEM) supplemented with 10% fetal bovine serum (FBS), 1× Antibiotic-Antimycotic solution

containing penicillin, streptomycin, and amphotericin, and 1× GlutaMAX (Gibco™, Thermo Fisher Scientific, Waltham, MA, USA) until they reached 80–90% confluency. The homogenized brain and lung tissues from case no. 1 were filtered through a 0.45 µm pore-sized membrane using a syringe filter and then diluted five-fold with viral growth medium (MEM supplemented with 2% FBS, 1× Antibiotic-Antimycotic solution, and 1× GlutaMAX). The Vero cell monolayer in a 12-well tissue culture plate was inoculated with 200 µl per well of the diluted, filtered samples. Virus adsorption was achieved by incubating the cells at 37 °C under a 5% CO₂ atmosphere for 1 h. The inoculum was then removed, and 1 mL of viral growth medium was added to each well. The cells were incubated at 37 °C under a 5% CO₂ atmosphere and observed microscopically for cytopathic effect (CPE) daily for 5–6 days post infection (DPI). Two blind passages were performed. Supernatants from CPE-positive wells were collected and stored at – 80 °C for further TMUV-specific RT-qPCR confirmation. Cell pellets were collected by centrifugation for 5 min at 200 × g, washed three times with PBS, and fixed in 2.5% glutaraldehyde solution at 4 °C overnight. Virus isolation was performed in duplicate, with mock-infection serving as a negative control. The fixed cells were then subjected to transmission electron microscopy (TEM) analysis.

Transmission electron microscopy

The glutaraldehyde-fixed Vero cells at 5 DPI were subjected to TEM analysis. Briefly, the cells were resuspended, triple-washed with 0.1 M PBS, and incubated with 1% (v/v) osmium tetroxide (OsO₄) for 1 h. The cells were then dehydrated in acetone and embedded in epoxy resin. The resin was sectioned, placed on a copper grid, and post-stained with 5% uranyl acetate. The ultrathin sections were examined under a TEM machine (HT7800, Hitachi, Tokyo, Japan) operating at 80 kV⁴³.

Immunohistochemistry

All FFPE tissues from both investigated and retrospective cases that tested positive for TMUV-specific RT-qPCR were subjected to horseradish peroxidase (HRP)-based IHC to localize TMUV. Briefly, the FFPE tissues were sectioned at 4 µm thickness and placed on positively charged slides. These slides were deparaffinized and rehydrated through serial dilutions of xylene and alcohol. Antigen retrieval was performed by autoclaving the sections with citrate buffer (pH 6) at 121 °C for 5 min. Endogenous peroxidase activity was blocked using 3% (v/v) hydrogen peroxide in absolute methanol for 15 min at room temperature. Non-specific binding was inhibited by incubating the sections with 2.5% (g/v) bovine serum albumin at 37 °C, 1 h in a moist chamber. The primary antibody, a purified mouse monoclonal against the flavivirus group antigen (clone D1-4G2-4-15), was applied at a 1:500 dilution and incubated overnight at 4 °C. After triple washes with 1× PBS, HRP-conjugated Envision polymers were applied as a secondary antibody. Detection of antigen-antibody complexes was achieved with a 1:100 dilution of 3, 3'-diaminobenzidine (DAB), with a positive reaction indicated by brown staining within the cellular morphology. JEV-infected brain section⁴⁴ and TMUV-RT-qPCR positive brain sections of case no.1 treated with normal rabbit IgG antibody NI01 (Sigma-Aldrich, MO, USA) served as positive and negative controls, respectively. In addition, FFPE brain section from the necropsied dolphin that tested negative for TMUV by qPCR incubating with the flavivirus-specific antibody, were used as additional negative controls.

Furthermore, IHC targeting CD3, CD79, CD20, and ionized calcium binding adaptor molecule 1 (Iba-1) was performed to assess the inflammatory process within brain lesions. Dual labelling for TMUV antigen and brain-specific cellular markers—neuronal nuclei (NeuN), glial fibrillary acidic protein (GFAP), oligodendrocyte transcription factor 2 (Olig-2), and Iba-1 that was specific to neurons, astroglia, oligodendroglia, and microglia, respectively—was performed to determine the cellular localization of TMUV in brain tissues. Double-labelling protocols followed previously established methods⁴⁵. A PermaRed AP chromogen (Diagnostics Biosystem, CA, USA) and StayGreen AP/Plus (Abcam, MA, USA) was used as the chromogen for NeuN and Olig-2 and GFAP and Iba-1 detections, respectively.

Results

Detection of TMUV in dolphins

Due to negative results from routine virologic tests and PCR for *T. gondii*, and the absence of morbillivirus antigen in the FFPE samples, the homogenized brain and lung tissues from case no. 1 were subjected to a metagenomic study using high-throughput sequencing. This analysis identified the presence of the TMUV genome. A 10,963-bp TMUV genome was recovered and submitted to the GenBank database under accession no. PQ154625. To validate the high-throughput sequencing results, RT-qPCR targeting TMUV was performed, which yielded positive results in all three dolphins (Table 1). The partial genome sequences obtained via RT-qPCR showed 100% nucleotide similarity with the TMUV sequence from the metagenomic study. Genomic analysis of the complete TMUV genome revealed 98.95% nucleotide similarity to the TMUV strain YN2020 (OQ238827.1) found in mosquitoes in China. Unique deduced amino acid mutations in the E gene of TMUV identified in dolphins were observed at N522H, V775M, M1168V, Y1618H, L2080I, and T2790I. Phylogenetic analysis placed the TMUV detected in dolphins within TMUV cluster 3, showing close genetic relationship to the TMUV strain YN2020 from mosquitoes in China (Fig. 1A).

In the investigation of TMUV in archival samples, RT-qPCR detection revealed a ~148-bp nucleotide sequence of TMUV in 3 out of 9 FFPE samples from captive dolphins that died in 2019 (Table 1). Although attempts were made to assess the genetic relationship between dolphin-TMUVs from archival samples and other TMUV strains, only 148-bp sequences of the TMUV E gene were recovered from the FFPE samples. Phylogenetic analysis based on these 148-bp sequences indicated that the TMUV detected in dolphins clustered within TMUV cluster 3 (Fig. 1B).

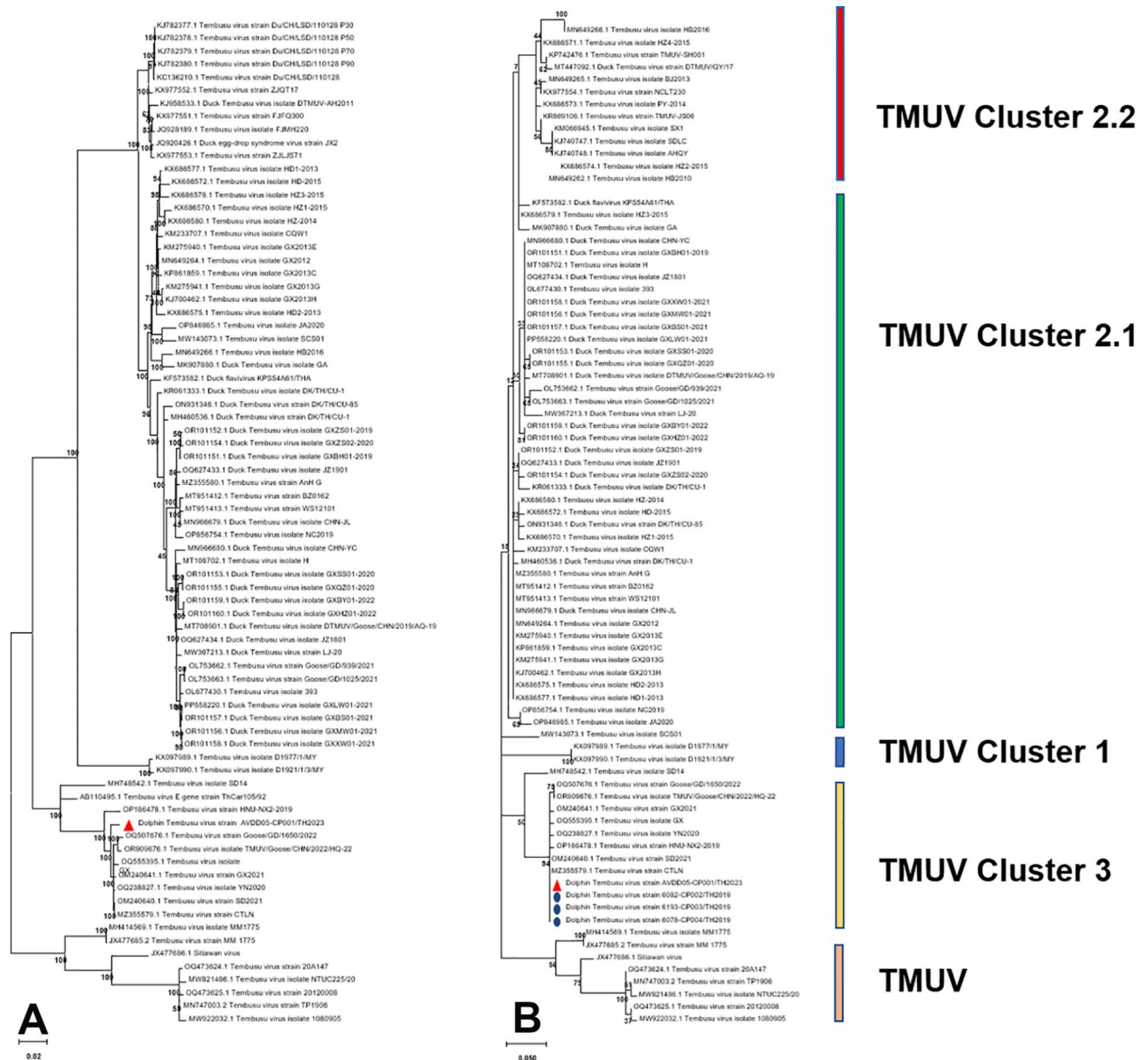


Fig. 1. Phylogenetic analysis of Tembusu virus (TMUV) identified in dolphins. Phylogenetic topology based on whole genome sequences (**A**) and partial NS2A gene sequences of TMUV (**B**) indicates that TMUV identified in dolphin no.1 (red triangle) is clustered within TMUV cluster 3. The TMUV sequences obtained from dolphins in archival samples (blue circles) also fall within cluster 3, closely related to the TMUV identified in this study. Bars indicate phylogenetic distance.

Histopathology of TMUV-infected dolphins

All brain specimens obtained from the three dolphins (case nos. 1–3) displayed non-suppurative encephalitis characterized by lymphoplasmacytic perivascular cuffing and gliosis, though the severity varied between individuals. The primary findings included minimal to moderate perivascular infiltrations of lymphocytes, with fewer plasma cells and rare foamy histiocytes forming cuffs of 1–10 layers (Fig. 2A). Aggregates of eosinophilic proteinaceous globules were observed around rare blood vessels in case nos. 1 and 2. Multifocal areas of rarefaction containing glial cell aggregates, few foamy histiocytes, occasional perivascular hemorrhages were present (Fig. 2B). Clusters of glial cells, sometimes associated with neurons, were observed, consistent with gliosis as defined by species-specific criteria. The meninges, where present, were variably expanded and contained pools of erythrocytes, sometimes disrupting the underlying neuropil. In case no. 3, perivascular cuffing and gliosis were less pronounced. Additionally, within TMUV-positive archival samples (case nos. 7–9), similar lesions were observed, including non-suppurative encephalitis with varying degrees of lymphoplasmacytic perivascular cuffing and gliosis. Morphologic diagnoses for these lesions are summarized in Table 1.

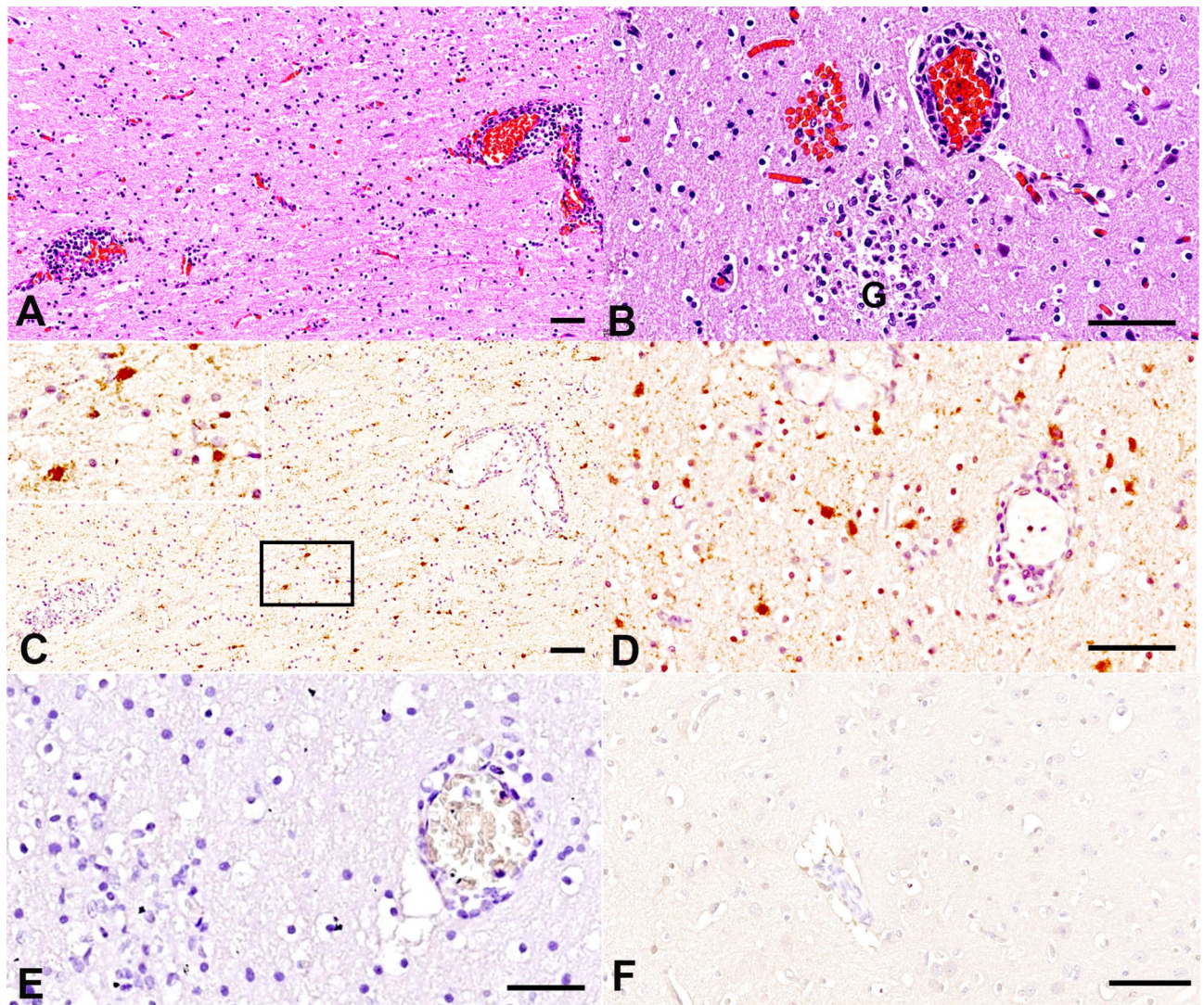


Fig. 2. Tembusu virus (TMUV) infection in dolphins. Cerebrum. case no. 1 (A–E), case no. 4 (F). (A) Two-three layers of non-suppurative perivascular cuffing are observed. (B) Focal perivascular non-suppurative encephalitis and gliosis is found. Hematoxylin and eosin. (C) TMUV antigens (brown color) are detected in the glial and neuron cells (inset). Immunohistochemistry (IHC). (D) Prominent nuclear and cytoplasmic labelling of TMUV antigen in neurons and glial cells are observed. (E) No positive reaction is observed in case no. 1 following incubation with normal rabbit IgG antibody (internal negative control). (F) no immunolabeling is detected in the TMUV-negative brain section incubated with purified mouse monoclonal antibody against the flavivirus group antigen (external negative control). G: gliosis. Scale bars indicate 20 μ m.

Histopathologic analysis of the kidney and lung from TMUV-positive case no. 1 revealed lesions likely unrelated to TMUV infection and potentially representing background changes. In the kidney, marked multifocal suppurative pyelonephritis and multifocal lymphoplasmacytic interstitial nephritis with prominent interstitial fibrosis were observed. Moderate renal congestion was observed in case no. 2. In the lung of the case no. 1, regional pulmonary fibrosis with diffuse pulmonary congestion and edema was found. However, these changes were not observed in lung sections from other TMUV-positive cases. No significant histopathologic changes were observed in organs other than the brain, kidney, and lung in case no. 1. Additionally, no significant lesions were observed in the lung or kidney of case no. 3 or in archival tissue samples (case nos. 7–9), except for the lesions detailed in the brain.

TMUV loads and distribution in deceased dolphins

TMUV loads and tissue distribution were determined using RT-qPCR. In dolphin no. 1, the highest viral loads were identified in the lung, brain, kidney, and spleen samples, respectively (Table 1). TMUV RNA was detected in the brain and kidney of case no. 2 and only in the brain of case no. 3. No TMUV RNA was identified in other organs. Due to the availability of only FFPE brain tissue of TMUV-positive archival samples, TMUV loads in other organs of these archival samples could not be determined. IHC-against TMUV antigen revealed positive

detection in the brains of all RT-qPCR-positive dolphins. TMUV was identified in cells resembling neurons and glial cells (Fig. 2C&D). No IHC signals identified in the negative controls (Fig. 2E&F). Furthermore, IHC-specific lymphocyte classification revealed that CD3-specific T lymphocytes were the main inflammatory cells within the perivascular cuffing of the brain tissue of TMUV-infected dolphins (Fig. 3A), but not CD20-specific B lymphocytes (Fig. 3B). To differentiate the TMUV-positive cells in the brain, dual labelling was performed, indicating that the TMUV antigens were localized in neurons and astroglia (Fig. 3C&D), but not in oligodendroglia or microglia.

Isolation of TMUV and ultrastructural investigation

TMUV was successfully isolated using Vero cells (Supplementary Fig. S1). Microscopically, TMUV caused a CPE, characterized by cells rounding up and detaching. The presence of CPE was first detected at 3DPI and reached significant CPE formation at 5DPI. Viral media from inoculated cells were collected at 5DPI, and the viral RNA was identified using RT-qPCR. To confirmed the infection of TMUV in Vero cells, the cells at 5DPI were harvested and submitted for TEM analysis.

Ultrastructurally, TMUV-infected cells exhibited moderately damaged cellular architectures, including disrupted nuclear and plasma membranes, engorged cytoplasmic organelles, and condensed nuclear chromatin. Fused cells containing two or more nuclei were also evident (Fig. 4A). Within disrupted cells, cytoplasmic vacuolation with various-sized smooth vacuoles was observed. These vacuoles contained numerous 40–50 nm electron-dense or electron-lucent particles (Fig. 4A). Enveloped nucleocapsid particles were found within the Golgi apparatus and some cytosolic vesicles (Fig. 4B). The enveloped particles, measuring 60–70 nm, were also located near the plasma membrane (Fig. 4C). Virions were present in dilated cisternae of the endoplasmic reticulum (Fig. 4D). Exocytosis vesicles containing the enveloped particles were seen within the complete plasma membrane, and virions were released from the cells via a ruptured plasma membrane.

Discussion

Tembusu virus (TMUV) is an emerging flavivirus primarily known to infect avian species, causing significant morbidity and mortality in poultry, particularly ducks^{10,11,16,19,20,42,46}. This virus has rapidly spread across Southeast Asia, leading to substantial economic losses in the poultry industry. Recent discoveries have revealed that TMUV can also infect mammalian species, broadening the scope of its potential impact^{28,29}. The detection of TMUV infection in dolphins provides evidence supporting the possibility that TMUV may pose a threat to mammals. The detection of TMUV infection in dolphins provides evidence that this virus, typically associated with avian species, can infect mammals under certain circumstances. While the findings highlight an unusual

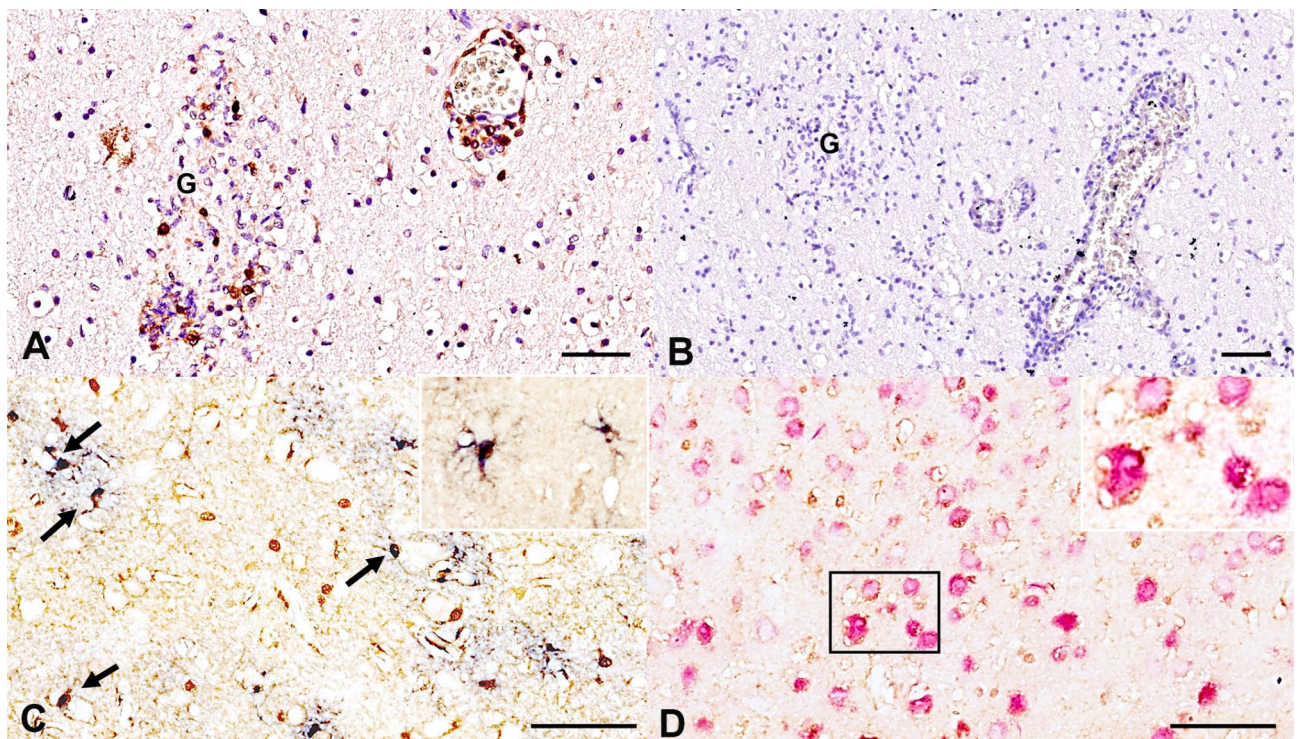


Fig. 3. Tembusu virus (TMUV) infection in dolphins. Cerebrum, case no. 1. (A) CD3-positive cells (brown color) are present in the areas of a perivascular cuffing and gliosis. (B) No immunoreaction observed in the section incubated with an antibody against CD20. (C) Co-localization (arrows) of TMUV antigen (brown color) and astrocyte (green color) (inset) (Dual IHC). (D) Co-labelling of TMUV antigen (brown color) and neuron-specific marker (red color) are identified (inset) (Dual IHC). G: gliosis. Scale bars indicate 20 μ m.

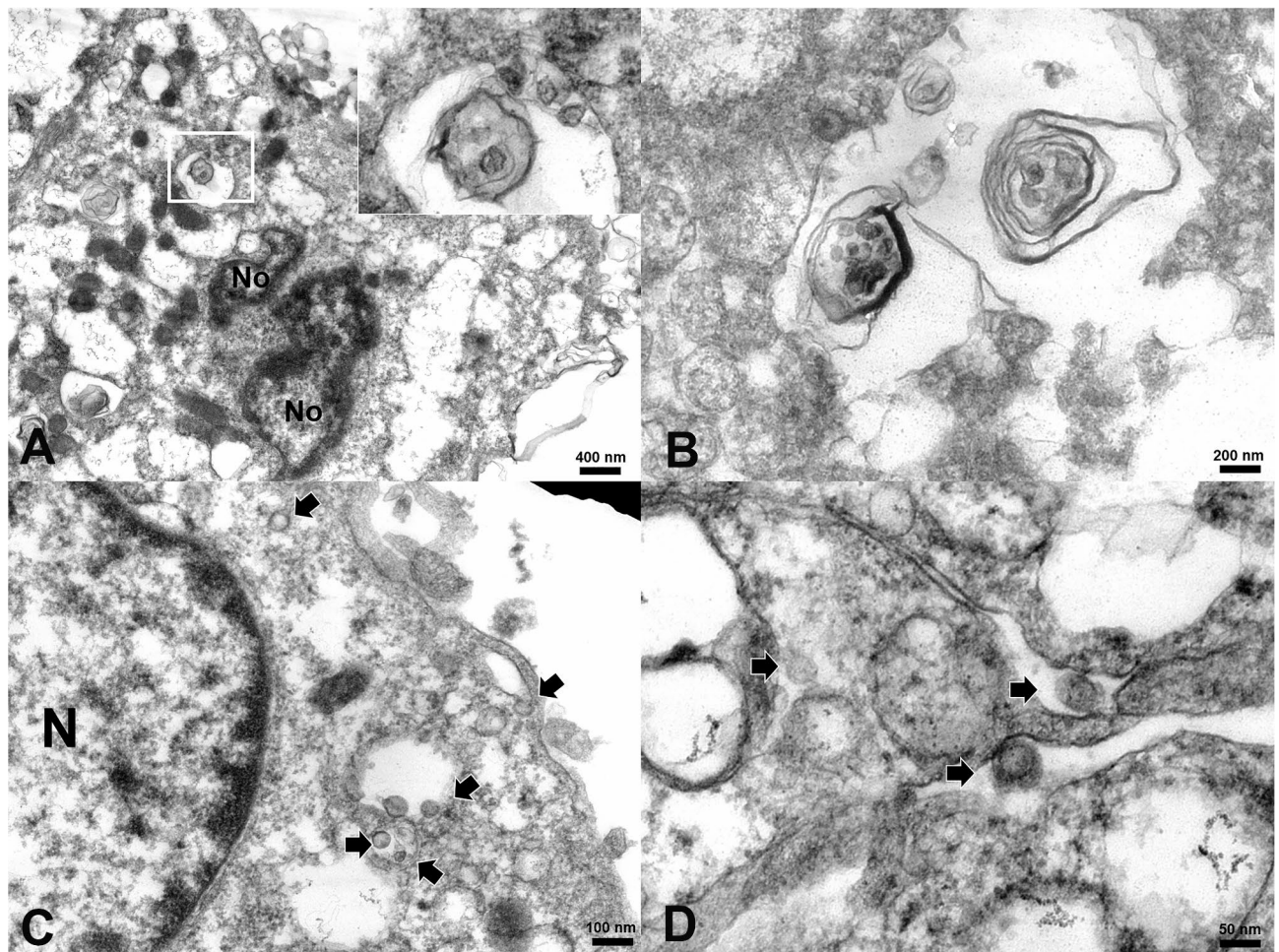


Fig. 4. Tembusu virus (TMUV) infection in Vero cell. Ultrastructural investigation of TMUV-infected Vero cell at 5DPI. (A) A cell presents cytoplasmic vacuolation. Within the vacuole, 50 nm-electron-dense particles were observed (inset). (B). Numerous viral particles are observed within the degenerated Golgi apparatuses of severely destructed cell. (C) There are electron-dense particles in the cytoplasm (arrows), and nearby the plasma membrane. (D) There are particles (arrows) present in the dilated cisternae of endoplasmic reticulum. No: Nucleolus; N: Nucleus. Scale bars indicate within the figures.

host occurrence, there is no evidence from this study to suggest broader cross-species transmission or infection within the zoo or natural surroundings. The identification of TMUV in dolphins suggests that the virus may have a wider host range than previously understood, warranting further investigation into its potential adaptability and ability to infect non-avian hosts. Given that these TMUV-infected dolphins resided in a zoo with many susceptible avian species, transmission could occur through various mechanisms. For instance, mosquitoes within the aquarium environment may transmit the virus. Infected mosquitoes could bite both avian and mammalian hosts, facilitating cross-species transmission^{30,47}. Additionally, other biting insects or contact with contaminated water sources could serve as potential transmission routes^{48,49}.

To adapt to and enhance infection in mammals, TMUV may undergo genetic mutations that allow it to overcome the species barrier. Several studies describe genetic mutations within the E protein of TMUV that may affect its ability to infect mammalian hosts. Although we did not find the mutations at positions 326, 156, and 154 of the TMUV E protein previously associated with mammalian infection^{50–52}, we identified other unique amino acid mutations in the TMUV-infected dolphins. It is important to acknowledge that these mutations could potentially represent adaptations arising from blind passaging in cell culture rather than genuine host-specific adaptations. Furthermore, no experimental methodologies were employed in this study to determine whether these mutations specifically enhance or limit the virus's infectivity in dolphin cells or other mammalian hosts. The functional implications of these specific mutations remain unclear and require further investigation to distinguish between cell culture artifacts and genuine host-specific adaptations.

The retrospective detection of TMUV in dolphins in Thailand since 2019 provides key insights into the virus's evolution, circulation, and phylogenetics. The identification of TMUV in dolphins, belonging to cluster 3 and closely related to mosquito strains from China, suggests notable evolutionary changes, host adaptation, and genetic diversity. Its presence in both dolphins and mosquitoes across distant regions highlights complex transmission dynamics, with mosquitoes likely playing a key role in dissemination. Detection since 2019

suggests ongoing circulation and a possible established transmission cycle. Additionally, the virus's presence in Thailand and China raises the possibility of long-distance dispersal through migratory birds, human activity, or environmental factors^{53–55}. Further investigation is needed to confirm the pathways facilitating this spread.

TMUV-infected dolphins exhibited neurological signs, with viral localization identified in brain tissue. While neurological lesions were observed and are consistent with findings in TMUV-infected avians and flavivirus encephalitis⁵⁶, the severity of these lesions was mild to moderate. Although several studies have indicated TMUV localization in neurons and glial cells²⁷, specific studies focusing solely on TMUV localization in glial cells are limited. This study, therefore, aims to identify the actual central nervous system (CNS) tropism of TMUV and the corresponding inflammatory response during natural infection. Apart from neurons, we found that TMUV exclusively localizes in astrocytes. The general behavior of flaviviruses, including TMUV, that can infect neurons and glial cells, mainly astrocytes, provides insights into how TMUV interacts with glial cells. Although CD3-positive T-cell lymphocyte perivascular cuffing is the main inflammatory process for TMUV-infected CNS dolphins, no TMUV was identified within the infiltrated lymphocytes. This suggests that the presence of CD3-T cells in perivascular cuffs may be a response to infected neuronal and glial cells, as flaviviruses generally do not infect T lymphocytes directly^{57,58}. This finding emphasizes the TMUV pathogenesis and may indicate the potential mechanisms of TMUV-induced CNS damage. It is important to acknowledge that the observed perivascular lymphocytic cuffing in the brain, while indicative of inflammation, is a non-specific finding that can be associated with a variety of systemic infectious processes of both bacterial and viral origin. Further experimental infection focusing on TMUV-induced CNS damage can elaborate our findings. Taken together, the kidney lesions observed in TMUV-positive case no. 1 may not be directly attributable to TMUV infection although the viral RNA was identified, as similar lesions were not identified in other TMUV-positive cases. Furthermore, the mixed nature of the kidney lesions—comprising both chronic (background) changes and acute alterations—suggests that the observed pathology may represent pre-existing conditions.

Despite high viral loads detected by RT-qPCR in the lungs of the infected dolphin (case no. 1), IHC failed to identify TMUV antigen. This discrepancy may be due to the higher sensitivity of RT-qPCR, which detects viral RNA even when protein levels are below IHC's detection threshold. Additionally, the FFPE process can degrade antigens, and uneven viral distribution may lead to sampling bias. The lung lesion observed, characterized by pulmonary fibrosis, likely represents a pre-existing chronic condition rather than an acute TMUV infection. Multiple examinations of the lung samples consistently yielded the same results, with RT-qPCR detecting viral RNA while IHC remained negative. This repeated outcome underscores the influence of technical limitations, sampling variability, and pre-existing pathology on diagnostic findings.

In conclusion, the detection of TMUV in dolphins, coupled with genomic and phylogenetic analyses, provides valuable insights into the virus's evolution, circulation patterns, and transmission to new species. These findings highlight the importance of integrated surveillance and research efforts to mitigate the impacts of emerging viral threats. Considering that TMUV infection exhibits fatal disease in dolphins, the detection of TMUV in diverse hosts underscores the need for a One Health approach, integrating human, animal, and environmental health efforts to address zoonotic disease threats.

Data availability

The data support the findings of this study are openly available in Tembusu virus isolate AVDD05-CP001/TH2023, complete genome at <https://www.ncbi.nlm.nih.gov/nucleotide/PQ154625>, reference number PQ154625.

Received: 4 October 2024; Accepted: 7 March 2025

Published online: 22 March 2025

References

- Lawrence, P., Heung, M., Nave, J., Henkel, C. & Escudero-Pérez, B. The natural Virome and pandemic potential: disease X. *Curr. Opin. Virol.* **63**, 101377. <https://doi.org/10.1016/j.coviro.2023.101377> (2023).
- Parkhe, P. & Verma, S. Evolution Interspecies transmission, and zoonotic significance of animal coronaviruses. *Front. Vet. Sci.* **8**, 719834. <https://doi.org/10.3389/fvets.2021.719834> (2021).
- Webby, R., Hoffmann, E. & Webster, R. Molecular constraints to interspecies transmission of viral pathogens. *Nat. Med.* **10**, S77–81. <https://doi.org/10.1038/nm1151> (2004).
- Escobar, L. E., Velasco-Villa, A., Satheshkumar, P. S., Nakazawa, Y. & Van de Vuerst, P. Revealing the complexity of vampire Bat rabies spillover transmission. *Infect. Dis. Poverty* **12**, 10. <https://doi.org/10.1186/s40249-023-01062-7> (2023).
- Chan, J. F., To, K. K., Tse, H., Jin, D. Y. & Yuen, K. Y. Interspecies transmission and emergence of novel viruses: lessons from bats and birds. *Trends Microbiol.* **21**, 544–555. <https://doi.org/10.1016/j.tim.2013.05.005> (2013).
- Simmonds, P. et al. ICTV virus taxonomy profile: flaviviridae. *J. Gen. Virol.* **98**, 2–3. <https://doi.org/10.1099/jgv.0.000672> (2017).
- Su, J. et al. Duck Egg-Drop syndrome caused by BYD virus, a new Tembusu-Related flavivirus. *PloS One*. **6**, e18106. <https://doi.org/10.1371/journal.pone.0018106> (2011).
- Platt, G. S. et al. Arbovirus infections in Sarawak, October 1968–February 1970 Tembusu and Sindbis virus isolations from mosquitoes. *Ann. Trop. Med. Parasitol.* **69**, 65–71. <https://doi.org/10.1080/00034983.1975.11686984> (1975).
- Kono, Y. et al. Encephalitis and retarded growth of chicks caused by Sitiawan virus, a new isolate belonging to the genus flavivirus. *Am. J. Trop. Med. Hyg.* **63**, 94–101. <https://doi.org/10.4269/ajtmh.2000.63.94> (2000).
- Homonay, Z. G. et al. Tembusu-like flavivirus (Perak virus) as the cause of neurological disease outbreaks in young Pekin ducks. *Avian Pathol.* **43**, 552–560. <https://doi.org/10.1080/03079457.2014.973832> (2014).
- Hamel, R. et al. New insights into the biology of the emerging Tembusu virus. *Pathogens* **10**, 475. <https://doi.org/10.3390/pathogens10081010> (2021).
- Huang, X. et al. Identification and molecular characterization of a novel flavivirus isolated from geese in China. *Res. Vet. Sci.* **94**, 774–780. <https://doi.org/10.1016/j.rvsc.2012.11.014> (2013).
- Yan, P. et al. An infectious disease of ducks caused by a newly emerged Tembusu virus strain in Mainland China. *Virology* **417**, 1–8. <https://doi.org/10.1016/j.virol.2011.06.003> (2011).

14. Hu, T., Wu, Z., Wu, S., Chen, S. & Cheng, A. The key amino acids of E protein involved in early flavivirus infection: viral entry. *Virol. J.* **18**, 136. <https://doi.org/10.1186/s12985-021-01611-2> (2021).
15. Yu, K. et al. Structural, antigenic, and evolutionary characterizations of the envelope protein of newly emerging Duck Tembusu virus. *PLoS One* **8**, e71319. <https://doi.org/10.1371/journal.pone.0071319> (2013).
16. Ninvilai, P., Tunterak, W., Oraveerakul, K., Amonsri, A. & Thontiravong, A. Genetic characterization of Duck Tembusu virus in Thailand, 2015–2017: identification of a novel cluster. *Transbound. Emerg. Dis.* **66**, 1982–1992. <https://doi.org/10.1111/tbed.13230> (2019).
17. Hamel, R. et al. Identification of the Tembusu virus in mosquitoes in Northern Thailand. *Viruses* **15** <https://doi.org/10.3390/v15071447> (2023).
18. Yu, G., Lin, Y., Tang, Y. & Diao, Y. Evolution of Tembusu virus in ducks, chickens, geese, sparrows, and mosquitoes in Northern China. *Viruses* **10** <https://doi.org/10.3390/v10090485> (2018).
19. Yu, Z. et al. Tembusu virus infection in laying chickens: evidence for a distinct genetic cluster with significant antigenic variation. *Transbound. Emerg. Dis.* **69**, e1130–e1141. <https://doi.org/10.1111/tbed.14402> (2022).
20. Yan, D. et al. The emergence of a disease caused by a mosquito origin cluster 3.2 Tembusu virus in chickens in China. *Vet. Microbiol.* **272**, 109500. <https://doi.org/10.1016/j.vetmic.2022.109500> (2022).
21. Tang, Y. et al. Characterization of a Tembusu virus isolated from naturally infected house sparrows (*Passer domesticus*) in Northern China. *Transbound. Emerg. Dis.* **60**, 152–158. <https://doi.org/10.1111/j.1865-1682.2012.01328.x> (2013).
22. Liao, J. Y. et al. Isolation and characterization of a novel Goose ovaritis-associated cluster 3 Tembusu virus. *Poult. Sci.* **102**, 102867. <https://doi.org/10.1016/j.psj.2023.102867> (2023).
23. Yang, Q. et al. Pathogenicity and interspecies transmission of cluster 3 Tembusu virus strain TMUV HQ-22 isolated from geese. *Viruses* **15**, 563. <https://doi.org/10.3390/v15122449> (2023).
24. Yurayart, N. et al. Pathogenesis of Thai Duck Tembusu virus in BALB/c mice: descending infection and neuroinvasive virulence. *Transbound. Emerg. Dis.* <https://doi.org/10.1111/tbed.13958> (2020).
25. Li, S. et al. Duck Tembusu virus exhibits neurovirulence in BALB/c mice. *Virol. J.* **10**, 260. <https://doi.org/10.1186/1743-422X-10-260> (2013).
26. Ti, J., Zhang, M., Li, Z., Li, X. & Diao, Y. Duck Tembusu virus exhibits pathogenicity to Kunming mice by intracerebral inoculation. *Front. Microbiol.* **7**, 190. <https://doi.org/10.3389/fmicb.2016.00190> (2016).
27. Yang, S., Shi, Y., Wu, J. & Chen, Q. Ultrastructural study of the Duck brain infected with Duck Tembusu virus. *Front. Microbiol.* **14**, 1086828. <https://doi.org/10.3389/fmicb.2023.1086828> (2023).
28. Ruangrun, K. et al. Analysis of Tembusu virus infection of human cell lines and human induced pluripotent stem cell derived hepatocytes. *Virus Res.* **292**, 198252. <https://doi.org/10.1016/j.virusres.2020.198252> (2021). <https://doi.org/>
29. Tang, Y. et al. Tembusu virus in human, China. *Transbound. Emerg. Dis.* **60**, 193–196. <https://doi.org/10.1111/tbed.12085> (2013).
30. Lensink, M. J., Li, Y. & Lequime, S. Aquatic flaviviruses *J. Virol.* **96**, e00439–e00422 <https://doi.org/10.1128/jvi.00439-22> (2022).
31. Jo, W. K. et al. An evolutionary divergent pestivirus lacking the N(pro) gene systemically infects a Whale species. *Emerg. Microbes Infect.* **8**, 1383–1392. <https://doi.org/10.1080/22221751.2019.1664940> (2019).
32. St Leger, J. et al. West Nile virus infection in killer whale, Texas, USA, 2007. *Emerg. Infect. Dis.* **17**, 1531–1533. <https://doi.org/10.3201/eid1708.101979> (2011).
33. van Boheemen, S. et al. A family-wide RT-PCR assay for detection of paramyxoviruses and application to a large-scale surveillance study. *PLoS One* **7**, e34961–e34961. <https://doi.org/10.1371/journal.pone.0034961> (2012).
34. Tong, S., Chern, S. W., Li, Y., Pallansch, M. A. & Anderson, L. J. Sensitive and broadly reactive reverse transcription-PCR assays to detect novel paramyxoviruses. *J. Clin. Microbiol.* **46**, 2652–2658. <https://doi.org/10.1128/jcm.00192-08> (2008).
35. VanDevanter, D. R. et al. Detection and analysis of diverse herpesviral species by consensus primer PCR. *J. Clin. Microbiol.* **34**, 1666–1671 (1996).
36. Li, Y., Meyer, H., Zhao, H. & Damon, I. K. GC content-based pan-pox universal PCR assays for poxvirus detection. *J. Clin. Microbiol.* **48**, 268–276. <https://doi.org/10.1128/jcm.01697-09> (2010).
37. Chang, C. Y. et al. The detection and association of canine papillomavirus with benign and malignant skin lesions in dogs. *Viruses* **12**, 85. <https://doi.org/10.3390/v12020170> (2020).
38. Jalal, S., Nord, C. E., Lappalainen, M. & Evengård, B. Rapid and sensitive diagnosis of *Toxoplasma gondii* infections by PCR. *Clin. Microbiol. Infect.* **10**, 937–939. <https://doi.org/10.1111/j.1469-0691.2004.00948.x> (2004).
39. Techangamsuwan, S. et al. Pathologic and molecular virologic characterization of a canine distemper outbreak in farmed civets. *Vet. Pathol.* **52**, 724–731. <https://doi.org/10.1177/0300985814551580> (2015).
40. Piewbang, C. et al. Domestic Cat hepatitis virus detection in blood and tissue samples of Cats with lymphoma. *Vet. Q.* **43**, 1–10. <https://doi.org/10.1080/01652176.2023.2265172> (2023).
41. Sun, Y. et al. Comprehensive evaluation of RNA and DNA viromic methods based on species richness and abundance analyses using marmot rectal samples. *mSystems* **7**, e0043022. <https://doi.org/10.1128/msystems.00430-22> (2022).
42. Huang, Y. et al. Chicken-origin cluster 3.2 Tembusu virus exhibits higher infectivity than duck-origin cluster 2 Tembusu virus in chicks. *Front. Vet. Sci.* **10**, 1152802. <https://doi.org/10.3389/fvets.2023.1152802> (2023).
43. Piewbang, C. et al. Dual infections of tilapia parvovirus (TiPV) and tilapia lake virus (TiLV) in multiple tilapia farms: their impacts, genetic diversity, viral tropism, and pathological effects. *Aquaculture* **550**, 737887. <https://doi.org/10.1016/j.aquaculture.2022.737887> (2022).
44. Piewbang, C. et al. Japanese encephalitis virus infection in meerkats (*Suricata suricatta*). *Zoonoses Public. Health.* <https://doi.org/10.1111/zph.12882> (2021).
45. Piewbang, C. et al. Naturally acquired feline bocavirus type 1 and 3 infections in cats with neurologic deficits. *Transbound. Emerg. Dis.* <https://doi.org/10.1111/tbed.14664> (2022).
46. Fang, Y. et al. Long-distance spread of Tembusu virus, and its dispersal in local mosquitoes and domestic poultry in Chongming Island, China. *Infect. Dis. Poverty.* **12**, 52. <https://doi.org/10.1186/s40249-023-01098-9> (2023).
47. Du, S. et al. Aedes mosquitoes acquire and transmit Zika virus by breeding in contaminated aquatic environments. *Nat. Commun.* **10**, 1324. <https://doi.org/10.1038/s41467-019-09256-0> (2019).
48. Nguyen-Tien, T., Lundkvist, A. & Lindahl, J. Urban transmission of mosquito-borne flaviviruses—a review of the risk for humans in Vietnam. *Infect. Ecol. Epidemiol.* **9**, 1660129. <https://doi.org/10.1080/2008686.2019.1660129> (2019).
49. Byas, A. D. et al. American alligators are capable of West Nile virus amplification, mosquito infection and transmission. *Virology* **568**, 49–55. <https://doi.org/10.1016/j.virol.2022.01.009> (2022). <https://doi.org/>
50. Liu, X. et al. 326K at E protein is critical for mammalian adaption of TMUV. *Viruses* **15**, 8563. <https://doi.org/10.3390/v15122376> (2023).
51. Peng, S. H. et al. Genome Analysis of a Novel Tembusu Virus in Taiwan. *Viruses* **2020**, 12. <https://doi.org/10.3390/v12050567> (2020).
52. Yan, D. et al. A single mutation at position 156 in the envelope protein of Tembusu virus is responsible for virus tissue tropism and transmissibility in ducks. *J. Virol.* **92**, 45. <https://doi.org/10.1128/jvi.00427-18> (2018).
53. Giesen, C. et al. A systematic review of environmental factors related to WNV circulation in European and mediterranean countries. *One Health* **16**, 100478. <https://doi.org/10.1016/j.onehlt.2022.100478> (2023).
54. Blahovec, M. R. & Carter, J. R. Flavivirus persistence in wildlife populations. *Viruses* **13**, 96. <https://doi.org/10.3390/v13102099> (2021).

55. Mackenzie, J. S., Gubler, D. J. & Petersen, L. R. Emerging flaviviruses: the spread and resurgence of Japanese encephalitis, West Nile and dengue viruses. *Nat. Med.* **10**, S98–S109. <https://doi.org/10.1038/nm1144> (2004).
56. Yang, S. et al. Tembusu virus entering the central nervous system caused nonsuppurative encephalitis without disrupting the blood-brain barrier. *J. Virol.* **95**, 36. <https://doi.org/10.1128/jvi.02191-20> (2021).
57. Sanchez Vargas, L. A., Mathew, A. & Rothman, A. L. T lymphocyte responses to flaviviruses—diverse cell populations affect tendency toward protection and disease. *Curr. Opin. Virol.* **43**, 28–34. <https://doi.org/10.1016/j.coviro.2020.07.008> (2020).
58. Grifoni, A. et al. T cell responses induced by attenuated flavivirus vaccination are specific and show limited Cross-Reactivity with other flavivirus species. *J. Virol.* **94**, 896. [https://doi.org/10.1128/\(2020\).jvi.00089-00020](https://doi.org/10.1128/(2020).jvi.00089-00020).

Acknowledgements

This research project is supported by The Chulalongkorn University, the Second Century Fund (C2F) (to C.P. and A.N.Z.), National Research Council of Thailand (NRCT): NRCT5-RGJ63001-013 and The Second Century Fund (C2F), Chulalongkorn University (to P.Po.), National Research Council of Thailand (NRCT): R. Thanawongnuwech TRF Senior Scholar 2022 #N42A650553 (to S.T.), and the National Natural Science Foundation of China (NSFC): Grant no. 32300424 (to L.Y.).

Author contributions

C.P., L.Y., and S.T. designed the study. C.P., A.N.Z., P.Po., L.Y., N.K. collected the samples and performed the experiments. C.P., L.Y., T.K., and N.K. analysed data. C.P., L.Y., A.N.Z., P.Po., and P.Pa. provided data collection. C.P. and L.Y. wrote the first draft of the manuscript and B.H. and S.T. finalized the manuscript. All authors approved the manuscript.

Competing interests

The authors declare no competing interests.

Ethics statement

All experimental protocols were approved by the Chulalongkorn University Care and Use Committee (no. 2431048). All procedures were done in accordance with the ARRIVE guidelines and regulations.

Additional information

Supplementary Information The online version contains supplementary material available at <https://doi.org/10.1038/s41598-025-93477-5>.

Correspondence and requests for materials should be addressed to S.T.

Reprints and permissions information is available at www.nature.com/reprints.

Publisher's note Springer Nature remains neutral with regard to jurisdictional claims in published maps and institutional affiliations.

Open Access This article is licensed under a Creative Commons Attribution-NonCommercial-NoDerivatives 4.0 International License, which permits any non-commercial use, sharing, distribution and reproduction in any medium or format, as long as you give appropriate credit to the original author(s) and the source, provide a link to the Creative Commons licence, and indicate if you modified the licensed material. You do not have permission under this licence to share adapted material derived from this article or parts of it. The images or other third party material in this article are included in the article's Creative Commons licence, unless indicated otherwise in a credit line to the material. If material is not included in the article's Creative Commons licence and your intended use is not permitted by statutory regulation or exceeds the permitted use, you will need to obtain permission directly from the copyright holder. To view a copy of this licence, visit <http://creativecommons.org/licenses/by-nc-nd/4.0/>.

© The Author(s) 2025